Available online at www.sciencedirect.com
ScienceDirect
Polymer 48 (2007) 3877–3882
polymer
www.elsevier.com/locate/polymer

Surface heterogeneity of a fluorinated block copolymer melt studied by a self-consistent-field analysis

Robert D. van de Grampel [a,1,2], Weihua Ming [a,2], Jozua Laven [a,2], Rob van der Linde [a,2], Frans A.M. Leermakers [b,*]

[a] *Laboratory of Coatings Technology, Materials and Interface Chemistry, Eindhoven University of Technology, P.O. Box 513, 5600 MB Eindhoven, The Netherlands*
[b] *Laboratory of Physical Chemistry and Colloid Science, Wageningen University, P.O. Box 8038, 6700 EK Wageningen, The Netherlands*

Received 13 February 2007; received in revised form 18 April 2007; accepted 19 April 2007
Available online 3 May 2007

Abstract

A two-gradient self-consistent-field theory using the discretisation scheme of Scheutjens and Fleer is applied to predict the structure in the lateral direction of the free surface of a microphase-separated compressible polymeric melt. A fluorinated block copolymer system is described in which parameters are chosen such that the fluorinated units preferentially segregate at the free surface. As soon as the copolymer architecture and interactions are such that the melt develops inhomogeneous structures (microphase separation), the surface also shows lateral inhomogeneities. Not only lateral changes in surface composition exist, but also indentations of the free interface are generated with a depth comparable to or smaller than the size of the segments that are enriched in the surface active component (fluorinated segments). These predictions are consistent with some earlier AFM investigations on fluorinated films. The system of choice presented in this paper is motivated by our experimental system but is not limited to this.

Keywords: Self-consistent field theory; Interfacial properties; Surface structure

1. Introduction

Fluorinated polymers are an interesting class of materials with exceptional properties like low surface energy, low friction coefficient, and hydrophobicity. These properties make this class of polymers interesting for coating applications. The surface energy of fluorinated polymers is associated with both the chemical composition (e.g. perfluoroalkyl chain) and the chain orientation at the surface. The pioneering studies of perfluorinated surfactants by Zisman [1] showed, for example, that a uniformly organized array of CF_3 groups creates a surface with a critical surface tension as low as 6 mN/m. Low surface tensions have been reported also for macromolecules with pendant perfluoroalkyl groups. Examples of such polymers are partly fluorinated polysiloxanes [2], polyacrylates [3], polymethacrylates [4], and polystyrene [5]. The pendant perfluoroalkyl chain introduced by the fluorinated monomer orients in the surface tilted with an angle to the substrate thus leading to low surface tension. Other polymer architectures like end-functionalized polymers [6] and block copolymers [7] were also employed to obtain fluorinated polymers with low surface tension.

Previously we analyzed the physical and thermodynamic properties of partially fluorinated polymethacrylate chains in the vicinity of the polymer melt–vapor interface [8]. Self-consistent-field (SCF) calculations showed a significant change in physical behavior when fluorinated units in the chains were grouped together forming a block structure. Even small blocks reduce the surface tension significantly. Besides, it was found that the polymer melt does not necessarily remain homogeneous. The results show that the stability of the

* Corresponding author. Tel.: +31 317 482268; fax: +31 317 483777.
E-mail address: frans.leermakers@fenk.wau.nl (Frans A.M. Leermakers).
[1] Present address: GE Plastics, Bergen op Zoom, The Netherlands.
[2] Fax: +31 40 2445619. E-mail: j.laven@tue.nl

0032-3861/$ - see front matter © 2007 Elsevier Ltd. All rights reserved.
doi:10.1016/j.polymer.2007.04.065

polymer melt with respect to microphase segregation depends non-monotonically on the length of the fluorinated block. For both very small and very long blocks the bulk will remain homogeneous, whereas for the blocks of intermediate length an inhomogeneous bulk may be formed. In these SCF analyses it was assumed that the system was homogeneous in the directions along the free surface.

The free surface of a copolymer melt is not necessarily chemically homogeneous. When spatial composition variations present themselves in the surface of a system, one may wonder whether this is an off-equilibrium effect, or a phenomenon that can be rationalized from equilibrium considerations. Unless there is a first-order surface phase transition, where exactly at the coexistence condition two phases with equal surface pressure exist side by side, a flat interface between polymer melt and air cannot tolerate lateral density gradients or surface composition variations that are larger than the equilibrium composition fluctuations. Typically, when the system is off-equilibrium there will be thermodynamic driving forces in the system that direct the system towards a stable equilibrium. In particular, density gradients in the lateral direction give rise to concomitant surface tension gradients. These surface tension gradients will push the system towards a laterally homogeneous surface.

The free surface has a unique alternative to deal with laterally inhomogeneous compositions, and thus laterally inhomogeneous interfacial tensions. It is not necessary that the free surface remains flat; it can develop 'hills' and 'valleys'. Such topological effects can subsequently be stable, i.e., in equilibrium, while the surface tension is still not homogeneous. Such surface topologies indeed can be found by tapping mode AFM analysis of fluorinated polymer [4a,9]. Nano-structured chemical heterogeneity in the surface was also observed using a light tapping force [10]. It is interesting to note that the 'low spots' in the topographic images were suggested to be the domains that are fluorine-rich. Again, the question arises whether these topologies were transient structures or represented true equilibrium ones. Many more detailed questions may follow from this. For example, how can one envision that such interfaces can exist at a constant chemical potential for the polymer chains? Such questions can only be answered convincingly in a thermodynamically consistent, statistical mechanical analysis. Recently a dynamic SCF theory has been used to study the terrace formation in a nano-structured thin block copolymer films [11]. The strong point of this method is that transient structural information is available. However, there is no insight into the long time effects because the authors stopped the simulations before the full relaxation took place. It might therefore have been the case that the terrace formation found is the result of a dewetting effect in progress. Again a thermodynamic study as presented below is necessary to be conclusive about the thermodynamic status of a system. A similar dynamic SCF approach has been used by Doi and coworkers [12]. These authors discuss how a mixture of two homopolymers phase separate bringing one of the components to the surface (heteronucleation). This leads also to lateral inhomogeneous surface structures.

In this paper we will focus on copolymer melts with a non-trivial interfacial behavior. In particular we will use the mean-field description of inhomogeneous polymer systems with the Edwards' diffusion equation as the fundamental starting point [13]:

$$\frac{\partial G(r,N)}{\partial N} = \frac{1}{6}\nabla^2 G(r,N) - u(r)G(r,N) \tag{1}$$

where $G(r,N)$ denotes the probability distribution of finding the end segment N of a polymer chain at coordinate r. This equation must be complemented with boundary conditions and a compressibility relation. Solutions of Eq. (1) can only be generated numerically and in such a procedure one typically makes use of lattice approximations. Here the method of Scheutjens and Fleer [14] is applied to solve Eq. (1) accurately. These authors used just one fundamental length, i.e., the size of a lattice site. The polymer chain is modeled as a string of flexible segments each with the same characteristic size, so that they fit on the lattice (one lattice site thus corresponds to about 0.5 nm in real space). The use of Eq. (1) implies that the chain Hamiltonian is that of a freely jointed chain (i.e., back folding is allowed). In fact two neighboring segments along the chain must occupy neighboring sites on the lattice, but longer-ranged positional correlations along the chain are ignored. The statistical weight of each conformation is found as the Boltzmann weight featuring the total potential felt by such conformation. The total potential is just the sum of potentials felt by each of its segments. The potentials are a function of the distribution of the molecules and for this reason they are often referred to as the self-consistent potentials. They are a functional of the volume fractions and parameterized by the short-range nearest-neighbor exchange energy parameters of the Flory–Huggins type. The Green's function $G(r,N)$ that obeys Eq. (1) is just the sum of these statistical weights over all possible and allowed conformations. Combination of complementary Green's functions, starting from opposite chain ends, gives access to the measurable volume fraction distributions $\varphi(r)$ of all segments. To put it differently, the normalization of the full set of statistical weights of all conformations gives access to the volume fraction distributions.

Here we will supplement the Edwards' equation with a compressibility condition that the total volume fraction of the polymeric component plus that of so-called vacancies add up to unity: $\varphi_P(r) + \varphi_V(r) = 1$. The phase rich in vacancies will be called the vapor. In the vapor phase, sufficiently far from the polymer phase, we position the system boundaries. At these boundaries we implement reflecting (mirror-like) boundary conditions (see Fig. 1). The melt–vapor interface is not affected by this boundary condition. As a result the interface is completely free, i.e., we do not impose any constraint on its topology or composition.

In order to study inhomogeneous interfaces, it is necessary to allow for at least two spatial coordinates. The Green's function must now depend on two coordinates: in this case x and z, $G(r,N) \rightarrow G(x,z,N)$ (see Fig. 1). The mean-field approximation is then applied in the y-direction. This means that in

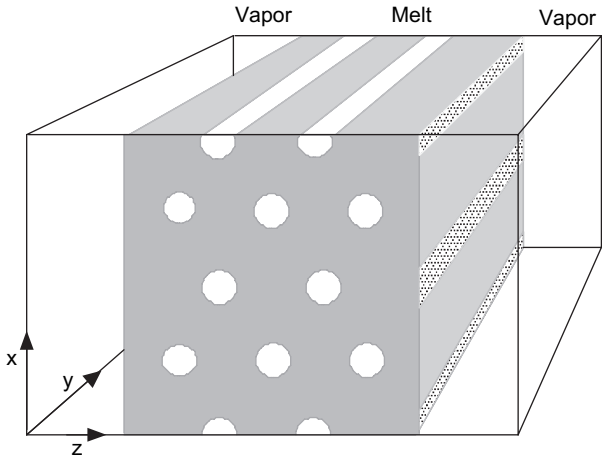

Fig. 1. Schematic representation of a thin film of a block copolymer melt that is microphase segregated in a hexagonal phase. The melt surface is along the $x-y$ plane. The $x-z$ plane is a perpendicular cut through the thin film. The cylinders are F-rich domains whereas the gray body is hydrocarbon-rich (F-poor) medium. On both the left and the right side the melt–vapor surface is present. The shading at the surface represents the expected surface density inhomogeneities.

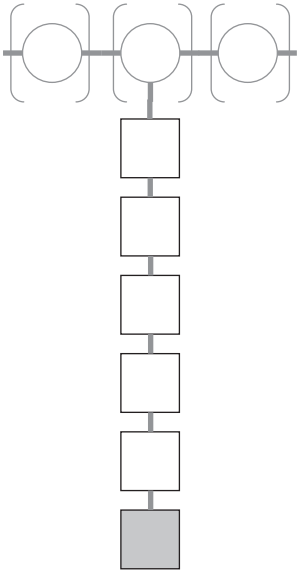

Fig. 2. A representation of the polymer used in this study. The circles represent the methyl methacrylate (**M**) units, the open squares are the CF_2 groups and the gray square is the CF_3 where $\chi_{CF_2,V} = \chi_{CF_3,V}$ ($\equiv \chi_{FV}$).

the y-direction the density variations are ignored and, related to that, the self-consistent potential $u(r,N) \rightarrow u(x,z,N)$ will be homogeneous in the y-direction. Solutions of this differential equation are generated numerically by the Scheutjens–Fleer formalism. Details of the numerical scheme may be found elsewhere [14]. The results of this theory are equilibrium density profiles $\varphi(x,y)$ (without random thermal fluctuations) as well as accurate data for thermodynamic variables.

Leibler [15] already showed that, for a block copolymer, the chain composition and the product of the chain length and the Flory–Huggins parameter χ determine whether the melt remains isotropic or microphase segregated. For the symmetrical diblock copolymer, the critical condition is $\chi^{cr}N = 10.5$. For asymmetric block copolymers the critical condition moves to higher values and the microphase topology becomes non-lamellar. In this paper, we will concentrate on an ABA block copolymer system with A being a methyl methacrylate unit (**M**) and B composed of one **M** unit and six fluorocarbon units ($\mathbf{F}_6$, $-(CF_2)_6F$; see Fig. 2). We assume that a hexagonal phase will form for large values of χ_{FM}. Such hexagonal phase can be captured in the coordinate system mentioned above. While the interest will be in the structural properties of the free surface, it is necessary to take into account the free volume in the system. As before, the polymer melt–vapor (V) interface will spontaneously form when both $\chi_{MV} > 0.5$ and $\chi_{FV} > 0.5$. The surface affinity of fluorinated groups is higher than that of the methacrylate units. Accordingly it is taken that $\chi_{MV} - \chi_{FV} > 0$. At fixed surface affinities, only the χ_{FM} parameter can be used to generate fundamentally different conditions. For large value of χ_{FM} the bulk becomes inhomogeneous, whereas for small values the bulk remains homogeneous. The idea of this work is to discuss the properties of the interface of the copolymer melt in these two regimes.

2. Results and discussion

In previous studies [16] it has been shown that the presence of perfluoroalkyl side chains in a polymethacrylate polymer lowers the surface tension of the polymer melt. Small amounts of these fluorinated side chains were found to cause a significant reduction of the surface tension. A detailed SCF analysis revealed that at a fixed composition (i.e., fixed number of perfluoroalkyl side chains), the surface tension reduction is maximized when the side chains are organized in a single block [8]. In that SCF analysis it was assumed that the system was homogeneous parallel to the free surface. In such an approach it is possible to reduce Eq. (1) to a one-dimensional differential equation. The advantage of the computer time reduction involved is that many molecular details can be included in the modeling. The present problem, as formulated in the previous section, calls for a two-dimensional gradient analysis. This has serious consequences with respect to the numerical analysis. In particular, due to both CPU limitations and increased memory requirements, it is not possible to describe the system in all molecular details. The simplification of the system must be such that the main characteristics are kept. We have chosen the following molecular structure: $(\mathbf{M})_{50}-(\mathbf{M}[\mathbf{F}_6])_3-(\mathbf{M})_{50}$, where the units **M** and **F** have been specified above and the square brackets indicate that the $\mathbf{F}_6$ segment is a side chain of the M-homopolymer. The main chain thus is $N_M = 103$ segments long (Fig. 2).

The free volume was modeled as vacancies that are denoted as V. Therefore there are three relevant Flory–Huggins interaction parameters. The interactions of **M** and **F** with V were fixed throughout this work: $\chi_{MV} = 2$ and $\chi_{FV} = 1.2$. The difference between these two χ values reflects that the F group is more surface active than the **M** group. The parameter χ_{MF} controls the microphase segregation of the melt. It was found

that the critical value of χ_{MF}^{cr} is about 0.53, below which the melt is homogeneous and above which it is in a hexagonal phase. We will present and discuss two typical results, one with a homogeneous bulk and the other with a structured bulk.

Calculations were performed in a 'box' with fixed dimensions. Both in the x- and the z-direction mirror-like, reflecting boundary conditions were implemented. The dimension of this 'box' was not chosen arbitrarily, but such that the film thickness is commensurate with the unit cell dimension found in a separate bulk calculation (not shown). The dimension of the box in the z-direction was chosen to be 70 lattice units. The amount of polymer (θ, in number of segments per unit length in the y-direction) in the system was fixed at $\theta = 655$. This resulted in a polymer film with a thickness of about 60 (lattice) sites and a size of the V-phase of 10 sites. Taking into account that there are reflecting boundary conditions in the y-direction, the total film thickness is 120 lattice units. The total film thickness was large enough so that the surface effects have just faded away in the center of the film. One would be inclined to increase the film thickness to be sure that there are no adverse effects of the finite size of the system, but this would lead to larger computation times and more importantly this would exceed the memory capabilities of our computer.

Intuitively one would expect that the numerical solution of the problem is easiest when the bulk is homogeneous. Therefore, this case is discussed first. In Fig. 3 the density distribution of the fluorine segments across the polymer film is plotted for $\chi_{MF} = 0.5$, a condition that is very close to the critical χ as mentioned above. As expected the density profile peaks sharply at the polymer–vapor interfaces, i.e., near $|z| = 60$. In the center of the melt, the density is independent of z, indicating that the melt is in the homogeneous, isotropic state. However, there are a number of oscillations visible in the **F** density. These effects have been discussed in detail previously. In first-order approximation, the variation in the distribution of the **M** units is the inverse of that of the **F** segments. In the top view graph of Fig. 3 the density profiles are presented in the x–z plane. The gray-scale is indicative of the fluorine density. As can be seen, the melt–vapor interface is exactly homogeneous and flat. This means that there is no surface tension gradient in this case.

In Fig. 4 the distribution of the fluorine groups is given for the case that the bulk is no longer homogeneous, i.e., $\chi_{MF} = 0.7$. From the top view graph, where the density profiles in the x–z plane are presented, one can clearly observe that a hexagonal phase is present in the bulk (for clarity a slab of 48×140 sites is shown instead of the 12×70 box used in the calculations). More interestingly, the interface is not homogeneous. There are local density variations laterally along the interface, as well as corresponding height variations. Two fluorine-density profiles in the z-direction are plotted in the bottom part of Fig. 4. The cross-sections are chosen through the centers of the F-rich domains. In the core of the film the fluorine-rich domains are evenly spaced. However, near the interfaces a fascinating effect occurs associated with the shape of the interface. This can be better seen in Fig. 5 where the interfacial region is enlarged. From this it is seen that the fluorine-density profile across the interface along line 2 (see Fig. 4, top) has a slightly higher maximum than the one along line 1. The average position of the F groups

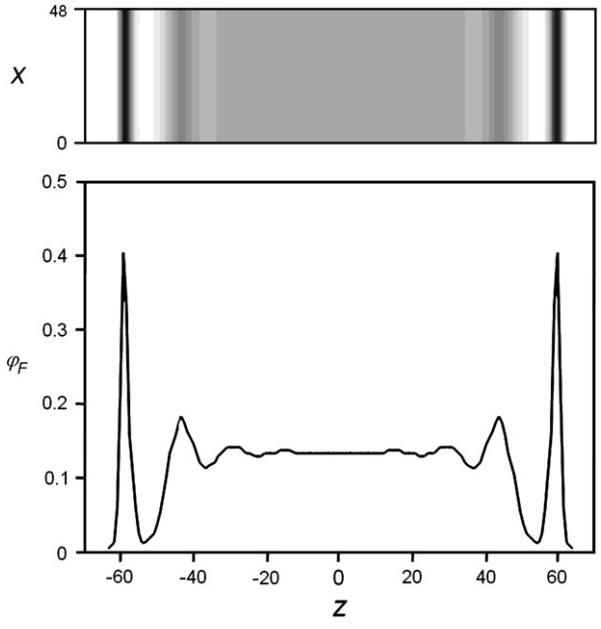

Fig. 3. Top: the two-dimensional density profile for a grid of 48×140 sites in the x–z plane of the **F** segments obtained from a calculation in a 12×70 box. The higher the concentration in **F** segments, the darker the gray scaling. Bottom: the corresponding volume fraction profile of the **F** segments across the film (in the z-direction). The two melt–vapor interfaces are found near $z = \pm 60$. The Flory–Huggins parameter for the **MF** interaction is $\chi_{MF} = 0.5$.

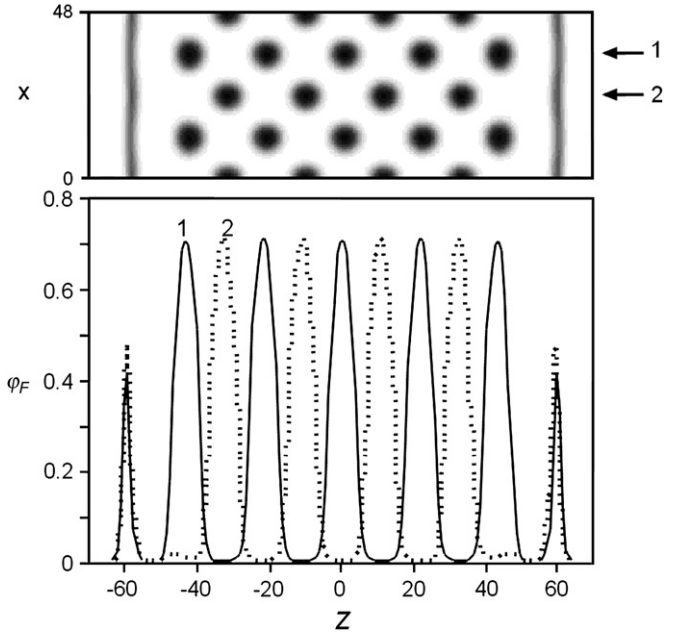

Fig. 4. Top: the two-dimensional density profile for a grid of 48×140 sites in the x–z plane of the **F** segments. The higher the fluorine concentration, the darker the gray scaling. Bottom: the corresponding volume fraction profiles of the **F** segments across the film (in the z-direction) along the path numbers 1 and 2, as indicated in the top view graph. The Flory–Huggins parameter for the **MF** contact is $\chi_{MF} = 0.7$. Other parameters are given in the text.

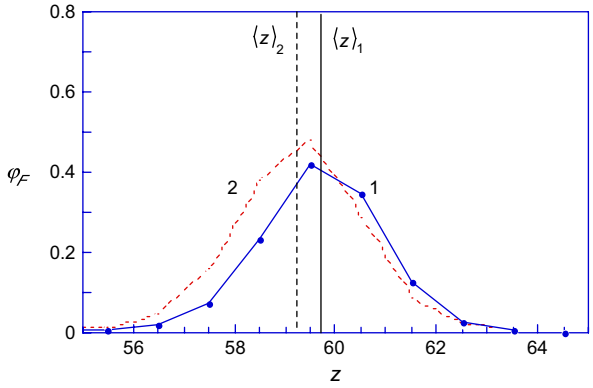

Fig. 5. Enlargement of the volume fraction profiles of the fluorine segments across the film (in the z-direction) near the melt–vapor interface. The vertical lines indicate the average positions of the fluorine groups (at the surface) along the lines 1 and 2.

near the interface, defined by the first moment, $\langle z \rangle = \sum_z z\varphi(z)/\sum_z \varphi(z)$, is also significantly displaced to smaller z values along line 2.

We conclude that it is possible to have a thermodynamically stable interface which is both non-flat and laterally inhomogeneous. The interfacial undulations are stabilized by the coupling of the interface to the bulk. This can clearly be seen from Fig. 4. Those F-rich domains that are near the surface are not all positioned at the same distance to the surface, i.e., along path number 2 the first F-rich domain is by ~50% further away from the surface than along path number 1. As the system tends to localize the fluorine-rich side chains in microphase segregated domains, the molecules near the surface where line 2 crosses (short: surface-2) are faced with the problem that no nearby fluorine-rich domains are available for the side chains to accommodate. Thus, without any adjustment within the system, the thermodynamic potential of these molecules would be raised along line 2 between the surface and the first fluorine-rich domain as counted from the surface. The system corrects for this mainly in two ways.

The first mechanism is that some molecules move away from this location at line 2, inducing a local indentation of the surface. This indentation at surface-2 decreases the local pressure P_2 in the polymer melt with respect to the gas phase from zero to a negative value $P_2 = \gamma_2/R_2$ where the surface tension γ and negative curvature $1/R_2$ are taken at surface-2. In turn, this induces a decrease in the local potential $\mu_2 = \mu(\varphi) + Nl^3P_2$ where l is the segment length and $\mu(\varphi)$ is the chemical potential found from local densities, e.g. by a Flory–Huggins type equation. An indentation at surface-2 must be matched by a bulge elsewhere, thus by a positive curvature $1/R_1$ at surface-1. This implies that the local thermodynamic potential just below surface-1 is raised. Both curvatures lead to a pressure difference in the melt of $\Delta P = \gamma_1/R_1 - \gamma_2/R_2$ when comparing the locations just below surface-1 and surface-2.

The second mechanism is that, after the action of only the first mechanism, the remaining molecules below surface-2 would still be left with part of the accommodation problem mentioned before, i.e., they are still faced with some "overdose" of fluorine-rich side chains. This is, at least partly, remedied by making the fluorine enrichment in surface-2 larger than in surface-1. This may lead to a lateral variation in the surface tension, with the lowest values probably located at surface-2. In passing we note that the fluorine-rich domains just beneath the interface do not have a perfect spherical shape but are somewhat elliptical. This is another manifestation of adaptation of the system to cope with the hexagonal packing of chains in the bulk and the macroscopic melt–vapor interface.

The differences in film thickness shown above are very small. From our results it is clear that the film thickness variations are triggered by an inhomogeneous bulk, i.e., it is a function of the value of χ_{MF}. We note, however, that the exact differences in film thickness that can be observed may also depend on the molecular structure of the polymers used, i.e., the availability of the phase segregated units to form domains. The small differences in film thickness indicate that the effect is not adversely affected by the underlying lattice. Indeed the interface shifts smoothly along the z-coordinate. We should realize that the case presented in Figs. 3 and 4 is still very close to the critical conditions. In most practical cases the copolymer systems can be much further away from these conditions and thus it is anticipated that this phenomenon can be experimentally observed. Indeed, we recently found that in partially fluorinated cross-linked polyurethane systems small patches of fluorine-rich domains are detectable by tapping mode AFM [10c]. The contrast in the phase image comes from different local stiffness of the F-rich domains. These domains are typically 2–3 nm 'below' the surface and with a lateral diameter of 15–20 nm. This phenomenon is consistent with some earlier findings on a fluorinated alkyd resin studied by Sauer and coworkers [10b]. More recently, Park et al. reported a hexagonally perforated surface layer for a PS-*b*-PMMA block copolymer melt [17]. These authors show that the structure inside the thin film has corresponding features as the surface layer, which is in good agreement with the current modeling study.

We would like to mention that our SCF method is not limited to the case of a fluorinated block copolymer system for which the fluorinated groups are side groups of an unfluorinated backbone. The self-consistent field method has been used extensively to microphase segregation in block copolymer melts and in principle for all such cases one can envision that a microscopically inhomogeneous bulk can couple to lateral inhomogeneous interfacial properties, where the free interface is both chemically inhomogeneous and has concomitant height variations.

3. Conclusions

Fluorine containing molecules typically accumulate at a polymer melt–vapor interface. Such low energy surfaces prevent subsequent adhesion of most, if not all, materials. A strategic approach to administer such fluorinated groups at the interface is to chemically link sufficient fluorinated units

to the polymer that forms the melt. However, in this case the macroscopically homogeneous polymer melt may develop some microphase-separated structure. In this paper it has been shown that when this happens, the free surface does not remain featureless. Lateral gradients in fluorine density are accompanied by height undulations of the free surface. In the F-rich regions the interface is indented and in the F-poor regions the interface has a 'small bump'. Such phenomena have been observed by AFM measurements and are now corroborated by a molecularly realistic self-consistent field theory.

Acknowledgements

This work was financially supported by the Dutch Organization for Scientific Research (CW-NWO) in the Priority Program for Materials Research (PPM).

References

[1] Zisman WA. In: Fowkes FW, editor. Contact angles, wettability and adhesion, ACS symposium series, vol. 43. Washington, DC; 1964.
[2] (a) Kobayashi H, Owen MJ. Trends Polym Sci 1995;3:10;
(b) Thorpe AA, Young SA, Nevell TG, Tsibouklis J. Appl Surf Sci 1998; 136:99;
(c) Perutz S, Wang J, Kramer EJ, Ober CK, Ellis K. Macromolecules 1998;31:4272.
[3] (a) DeSimone JM, Guan Z, Elsbernd CS. Science 1992;257:945;
(b) Guyot B, Ameduri B, Boutevin B. J Fluorine Chem 1995;74:233.
[4] (a) Schmidt DL, Coburn CE, DeKoven BM, Potter GE, Meyers GF, Fischer DA. Nature 1994;368:39;
(b) Kassis CM, Steehler JK, Betts DE, Guan Z, Romack TJ, DeSimone JM, et al. Macromolecules 1996;29:3247;
(c) Takahashi S, Kasemura T, Asano K. Polymer 1997;38:2107;
(d) Krupers M, Slangen P-J, Möller M. Macromolecules 1998;31:2552;
(e) Thomas RR, Anton DR, Graham WF, Darmon MJ, Sauer BB, Stika KM, et al. Macromolecules 1997;30:2883;
(f) Tsibouklis J, Graham P, Eaton PJ, Smith JR, Nevell TG, Smart JD, et al. Macromolecules 2000;33:8460.
[5] (a) Höpken J, Möller M. Macromolecules 1992;25:2482;
(b) Bouteiller V, Garnault AM, Teyssié D, Boileau S, Möller M. Polym Int 1999;48:765.
[6] (a) Albert B, Jerome R, Teyssié P. Macromol Chem 1984;185:579;
(b) Hunt Jr MO, Belu AM, Linton RW, DeSimone JM. Macromolecules 1993;26:4854;
(c) McLain SJ, Sauer BB, Firment LE. Macromolecules 1996;29:8211;
(d) Su Z, Wu D, Hsu SL, McCarthy TJ. Macromolecules 1997;30:840;
(e) Lee W-K, Losito I, Gardella Jr JA, Hicks Jr WL. Macromolecules 2001;34:3000.
[7] (a) Wang J, Mao G, Ober CK, Kramer EJ. Macromolecules 1997;30: 1906;
(b) Genzer J, Sivaniah E, Kramer EJ, Wang J, Körner H, Xiang M, et al. Langmuir 2000;16:1993;
(c) Zhang Z, Ying S, Zhang Q, Xu X. J Polym Sci Part A Polym Chem 2001;39:2670.
[8] Van de Grampel RD, Ming W, Laven J, van der Linde R, Leermakers FAM. Macromolecules 2002;35:5670.
[9] Schmidt DL, DeKoven BM, Coburn CE, Potter GE, Meyers GF, Fischer DA. Langmuir 1996;12:518.
[10] (a) McLean RS, Sauer BB. Macromolecules 1997;30:8314;
(b) Sauer BB, McLean RS, Thomas RR. Langmuir 1998;14:3045;
(c) Ming W, Tian M, van de Grampel RD, Melis F, Jia X, Loos J, et al. Macromolecules 2002;35:6920.
[11] Lyakhova KS, Horvat A, Zvelindovsky AV, Sevink GJA. Langmuir 2006; 22:5848.
[12] Morita H, Kawakatsu T, Doi M. Macromolecules 2001;34:8777.
[13] (a) Edwards SF. Proc Phys Soc London 1965;85:613;
(b) Dolan AK, Edwards SF. Proc R Soc London Ser A 1974;337:50.
[14] (a) Fleer GJ, Scheutjens JMHM, Cohen Stuart MA, Cosgrove T, Vincent B. Polymers at interfaces. London: Elsevier; 1993;
(b) Leermakers FAM, Scheutjes JMHM, Lyklema J. Biochim Biophys Acta 1990;1024:139;
(c) van der Linden CC, van Lent B, Leermakers FAM, Fleer GJ. Macromolecules 1994;27:1915;
(d) Wijmans CM, Leermakers FAM, Fleer GJ. Langmuir 1994;10:4514;
(e) Leermakers FAM, van den Oever JMP, Zhulina EB. J Chem Phys 2003;118:969.
[15] Leibler L. Macromolecules 1980;13:1602.
[16] Van de Grampel RD, Ming W, Gildenpfennig A, van Gennip WJH, Laven J, Niemantsverdriet JW, et al. Langmuir 2004;20:6344.
[17] Park I, Park S, Park H-W, Chang T, Yang H, Ryu CY. Macromolecules 2006.